

# Extraction and Simulation of Intra-gate Defects Affecting CMOS Libraries

Aymen Ladhar

STMicroelectronics, Ariana, Tunisia

Electronics, Micro-technology and Communication Laboratory, Sfax, Tunisia

Email: aymen.ladhar@ieee.org

Mohamed Masmoudi

Electronics, Micro-technology and Communication Laboratory, Sfax, Tunisia

Email: mohamed.masmoudi@enis.rnu.tn

**Abstract**—Shorts and opens are the most common type of defects in digital integrated circuits ICs. They can affect interconnect wires connecting gates or transistors inside. Tools targeting the extraction of these potential defects focus only on the inter-gate bridging faults, and no one presents a solution to extract potential intra-gate bridging faults, open and resistive-open defects. This paper presents an automated approach to extract and simulate potential intra-gate defects in standard cell library, based on the use of verification and simulation CAD tools. As application, we used these fault signatures to diagnose different types of intra-gate defects. Experimental results show the efficiency of our approach to isolate injected defects on industrial designs.

**Index Terms**— Intra-gate defects, extraction, simulation, layout analysis, fault diagnosis.

## I. INTRODUCTION

Nowadays, the world has been revolutionized by the rapid growth in the semi-conductor field. As the IC technology process becomes more complex and minimum feature size approaches nanometer range, manufacturing quality and yield are becoming more sensitive to physical defects, imperfection and process variations. These defects are not affecting only the interconnecting wires between gates but also transistors inside. The simulation of intra-gate faults is a challenging task. In fact, some of these defects can be sequence dependant, which means the test result depends on the ordering of the test patterns, even though the circuit is fully combinational. These defects can be also timing dependant, which means the test results change with the test speed [1].

Intra-gate defects can be classified on four main classes upon their electrical behavior when they are simulated:

- The first category is bridging fault that results from shorting two lines that must not be connected.
- The second category is source drain open or stuck-open fault [4] resulting from a complete break between circuit nodes that should be connected [5]. Stuck-open faults can cause sequential behavior and thus require a certain sequence of patterns in order to be detected. The first pattern excites the defect while the second one detects it. It has been shown in [1] that changing the test

speed, voltage and temperature, do not improve the test effectiveness. The stuck-open fault can be detected by stuck-at fault patterns at nominal condition.

- The third category is gate open defect resulting in a complete break in the transistor gate, the behavior of this fault is depending on the state of neighbored lines and parasitic capacitances and resistances [6].

- The last category of intra-gate defects is resistive-open defect that is defined as an imperfect circuit connection that can be modeled as a defective resistor between the circuit nodes that should be connected. The behavior of this fault depends usually on the test speed and the parasitic resistance value causing this defect [1]. It has been also shown that the optimal test voltage and test temperature depend on the defect location and defect material respectively.

The knowledge of layout topology is mandatory to have realistic simulation results of intra-gate defects. In fact, these defects are generally originated either by neighbored lines causing bridging faults, or by defective contacts causing open defects. In order, to precisely simulate intra-gate defects, it is mandatory to extract from the cell's layout all the neighbored lines as well as all the contact placements and transistors linked by each contact [27]. Previous works on neighbored lines extraction [2] [3] focused only on the extraction of neighbored metal wire connecting standard cell gates. This information is then used for bridging fault test pattern generation or for a realistic bridging fault diagnosis. To our knowledge, no works has been proposed for the extraction of intra-gate defects especially, defects caused by defective contacts. The knowledge of contact placements becomes mandatory for precise simulation. For example, it may happen that a single contact disconnects many transistors in the same time causing multiple open defects.

In this paper, we present an efficient methodology to extract all the potential intra-gate defects affecting standard cell libraries. Then we use this information to simulate these potential defects. Their fault signatures are then recorded in a fault dictionary. As application we use the created fault dictionary for an intra-gate diagnosis procedure [7] [8]. Our diagnosis methodology delivers more precise and realistic transistor level diagnosis results than [18]-[24]. In fact, the name of the shorted

lines in case of intra-gate bridging fault and the names of the disconnecting transistors in case of contact open or resistive-open defects are presented in diagnosis results. Previous works are not able to diagnose open defects when the defective contact disconnects more than one transistor. The algorithm proposed in this work can diagnose intra-gate defects in presence of multiple exercising conditions per pattern [24].

The rest of the paper is organized as follow. Section 2 explains how we proceed to extract intra-gate defects. Section 3 explains how we create an intra-gate fault dictionary containing all the fault signatures of all potential transistor defects caused by neighbored lines and defective contacts. In section 4 we present our methodology for intra-gate defects diagnosis. Experimental results are included in section 5, and finally conclusions are drawn.

II. OUTLINE OF THE METHODOLOGY

An overview of the proposed method to construct the fault dictionary containing all the potential intra-gate fault signatures is presented in figure 1. This fault dictionary is then used to diagnose intra-gate defects affecting standard cell libraries. The proposed method starts from the layout database to generate in the final step a fault dictionary containing the signatures of the entire intra-gate defects inside each library cell. Our algorithm begins by extracting all the neighbored lines inside those gates. Then, it determines the topology of nets inside it, in order to extract potential open and resistive open defects. In fact, these defects are generally affecting contacts, that link poly-silicon layer to metal layer, and diffusion layer to metal layer.

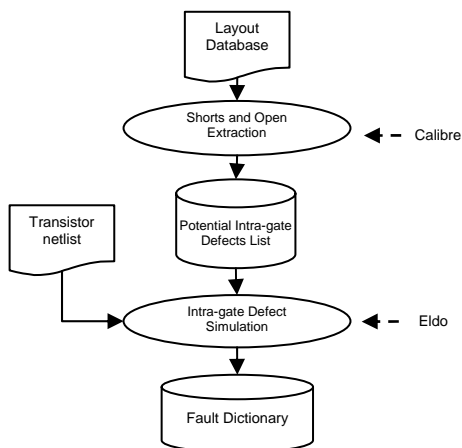


Figure 1. Overview of the method to create the fault dictionary

Once all the potential intra-gate defects are identified. They are injected in the transistor netlist and a post layout simulation is performed in order to determine their fault signatures. In the simulation, we consider all the possible input combinations and we take into account sequence dependant defects. All the simulation results are then collected in a fault dictionary. This fault dictionary is created only one time and then can be used for the

diagnosis of any circuit having the same technology as the library technology.

The extraction of transistor defects is performed using the verification CAD tool Calibre [9] [10]. However, the post layout simulation is performed using Eldo simulator [11]

III. EXTRACTION OF INTRAGATE DEFECTS

In this section, we focus on the extraction of potential bridging and open defects in the transistor level. For this purpose, each neighbored lines can be a potential bridging fault and each contact is a potential open or resistive open defect.

A. Layer definition

Before explaining our method to extract potential intra-gate defects, we explain in the following the method to define the (x, y) coordinates of each layer and transistor in the cell's layout.

A layer X is defined in the cell's layout by its (x, y) coordinates, and a transistor M is defined by the (x, y) coordinates of its poly-silicon gate.

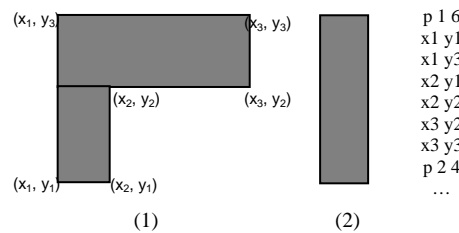


Figure 2. Layer definition

For example, figure 2 shows one layer composed by two shapes p1 and p2. The first one (1) p 1 is represented by 6 couples of coordinates, and the second one (2) p 2 is defined by 4 couples. The same figure 2 represents on the right side the way that the calibre query server presents these (x, y) coordinates of the shape (1).

B. Coordinates determination of potential intra-gate defects

The calibre SVRF rules enable the development of Design Rule Checks DRC and Layout Versus Schematic LVS checks. We are focusing on the following parts on the DRC checks. Those are used to determine the coordinates of contacts and neighbored lines. Actually, the calibre DRC rules allow computing the distance between each layout shape of the same layer (1) (2) and it compares the calculated distance to a certain Design For Manufacturing DFM distance fixed by the technology rules. The calibre DRC checks can calculate also the width of the different shapes like contacts in the layout database (3), and to compare it to a certain DFM distance fixed by the technology rules.

```

METAL_SPACING {
external M1i < DFM_M1
}
    
```

```

POLY_SPACING {
external POi < DFM_PO
}
    
```

```
Contact_SPACING {
internal COi < DFM_CO
}
```

(3)

The method used, to determine the (x, y) coordinates of all contacts and all the neighbored shapes in each cell, consists to modify the DRC rule file, where the DFM values are replaced by new once.

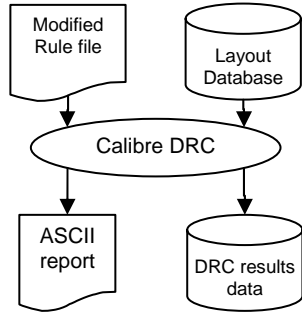


Figure 3. Calibre DRC

Figure 3 shows how we proceed to determine the coordinates of contacts and the neighbored shapes using Calibre DRC. In fact, it uses technology rules in the rule file to identify, check devices and connectivity in the layout database for any errors. In this process, DRC generates an ASCII report and a DRC results database, which are used to locate errors. As inputs calibre DRC has the layout database of the studied cell and a modified DRC rule file. The minimal distances between metals and poly-silicon shapes are equal to a new distance DFM fixed according the library technology. The minimum contact width is also changed to a new DFM value. Using a modified rule file we are able to collect at the end of this step the coordinates of all the contacts and the coordinates of all the neighbored shapes that can be metal shapes or poly-silicon shapes.

*D. Net names determination of the neighbored lines from (x, y) coordinates*

In the previous section, we explained the method to extract the coordinates of potential intra-gate defects. This information will be used next to identify the net name of each potential intra-gate defect using calibre query server. The calibre query server is a licensed database server allows the examination of the contents of the Standard Verification Database (SVDB) generated by LVS/LVS-H [10]. The calibre query server allows having the entire layers name in the (x, y) placements for metal and poly-silicon layers. However, the tool is not able to identify the net name corresponding to contacts's coordinates.

Figure 3 shows how we proceed with the calibre query server in order to obtain from (x, y) coordinates the net names of layers in these locations. As inputs, we introduce the coordinates of the neighbored shapes and the SVDB directory. As results, we collect all the net names of all the layers on each physical coordinates. The neighbored layers belong to the same net name are dropped from the list of neighbored lines.

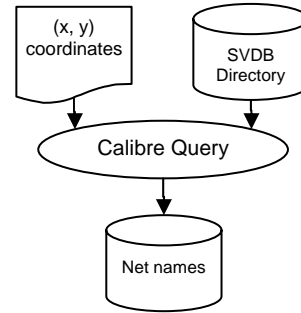


Figure 4. Net name extraction using Calibre query

*E. Open and resistive open extraction*

Contacts and vias are the main cause of open and resistive open defects in CMOS ICs. At the transistor level, we can only find contacts linking metal layer to poly-silicon or linking metal to diffusion layer. These connections are analyzed in the following to identify contact open defect's effects, i.e. transistors that are disconnected when an open contact defect occurs.

Figure 5 shows how we proceed to extract the topology of all the nets in the transistor netlist using the calibre query server. As inputs, we introduce the entire names of all the nets and transistors in the transistor netlist as the SVDB directory. As result we collect the (x, y) coordinates of all transistors, defined by the coordinates of these poly-silicon gates, thus the (x, y) coordinates of each layer constituting each net in the transistor netlist. Here we can distinguish 4 connection types:

- Case (1): A diffusion connection n or p: in this case the transistors are directly linked without contacts.
- Case (2): A metal-poly connection: in this case the two layers are connected by contacts. Each poly-silicon layer connects the gates of nMOS and pMOS transistor.
- Case (3): A metal-diff connection: in this case the metal layer connects the diffusion layer by contacts.
- Case (4): A diff-metal-poly connection: in this case the diffusion and metal layers are connected by contacts. The metal and poly-silicon layers are also connected by contacts. This kind of connection is used to connect the drain of transistors with gates of other transistors.

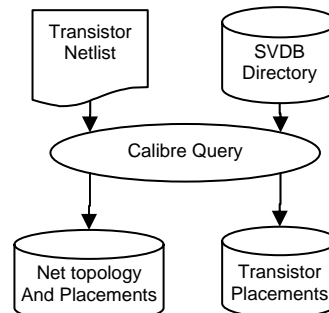


Figure 5. Net topology using Calibre query

The algorithm used to determine what transistors are disconnected in the transistor netlist, where an open defect caused by contacts occurs, is described in figure 6. From the net's topology we distinguish the type of connection. Here we focus on case (2), (3) and (4) since

these connections contain contacts. Each one of these connection contains either Metal-diffusion or Polysilicon-diffusion connection. For the Metal-diffusion connection we determine the number and the coordinates of each shape constituting the  $n$  and  $p$  diffusions. Then, we look for transistors that are linked to each one of these shapes. The transistors that are connecting to the same diffusion shape are linked by the same contact. The same algorithm is used for the Poly-Metal connection. Notice that if a layer is connected to another layer by more than one contact this net will not be analyzed. Since we suppose that an open defect cannot affect more than one times a net.

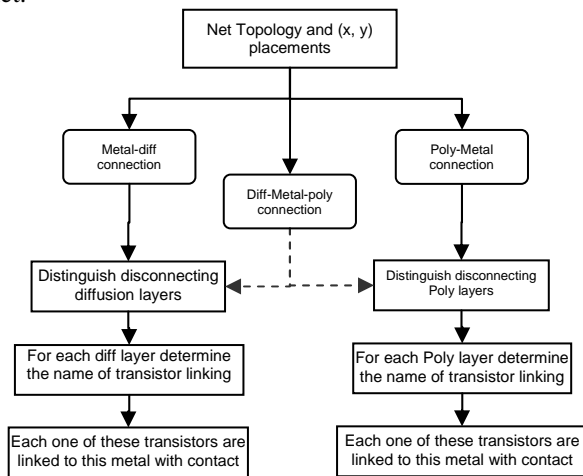


Figure 6. Contact extraction algorithm

**F. Full intra-gate defect extraction algorithm**

Figure 7 shows the full extraction algorithm. It begins by selecting a gate from the analyzed standard cell library. Then, it determines the coordinates of contacts and neighbored lines in each gate. Once this step is performed, the net name of each neighbored lines are determined. After this step, the contact extraction algorithm is launched. Finally, a list of all potential intra-gate defects is collected.

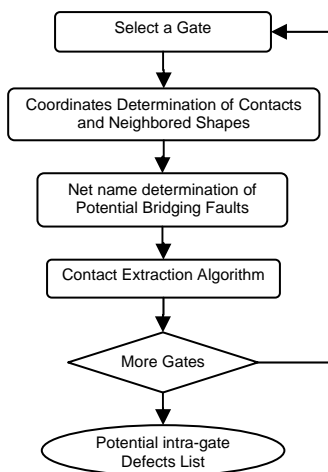


Figure 7. Full intra-gate defect extraction algorithm

**IV. MODELING AND SIMULATING INTRAGATE DEFECTS**

In this section, we describe how we proceed to simulate these potential intra-gate defects already extracted in the previous section. For this, we use a transistor netlist containing all the parasitic capacitances and resistances that have been extracted from the gate's layout. The simulation is done for each gate by injecting all potential intra-gate defects one a time. The simulation is done at nominal voltage. We simulate all the possible input combinations using the *vpattern* voltage source from the eldo library. The fault dictionary is structured like a truth table where the expected and the faulty value are mentioned for each input value and for each defective location.

**A. New transistor netlist construction**

Once all the neighbored lines and potential contact placements are identified, we perform a post layout simulation in order to collect their faulty signatures. The simulation is done with Eldo simulator [11]. For this purpose, a new transistor netlist is constructed. In this transistor netlist, each neighbored nets are linked by a resistance  $R_{BF}$  of  $1\text{ G}\Omega$ , each transistor gate is linked to their source and drain by a resistance of  $1\text{ G}\Omega$ . Indeed, it has been shown in [12] that the use of  $T_iS_{i2}$  can cause bridging faults between G-S and G-D. And finally, each contact is replaced in the transistor netlist by a resistance  $R_{OP}$  of  $1\Omega$ . The simulation of the transistor netlist with these new parameters gives the same results than the old one. But in modifying the value of one resistance we collect as response the signature of this fault on this location.

**B. Simulation of intra-gate bridging fault**

Intra-gate bridging fault results from shorting two nets or more inside a cell. To simulate a short between two neighbored lines we suppose that they are linked by a parasitic resistance of  $1\Omega$ . The simulation of different intra-gate bridging faults in different cells shows that:

- Some intra-gate bridging faults have the same effects than a stuck-at fault on one of the primary inputs or the output of the target gate.
- Some intra-gate bridging faults have no effect on the gate's primary output and the gate is kept faulty-free.
- Some intra-gate bridging faults drive the gate's primary output to the opposite value for some excitation values and keep the rest faulty free.

**C. Simulation of open defect**

Intra-gate open defects can be classified in two categories upon their location on the cell:

- Open source or drain also known as stuck-open fault.
- Open gate.

TABLE I. TRUTH TABLE OF A NAND 2 GATE

$Z_{Previous}$	A	B	$C_{Good}$	$C_{Faulty}$
0	1	0	1	0
1	1	0	1	1

The open source or drain defect assumes a particular transistor is permanently turned off, as a result, for example, of a failed transistor or connection break [1] [5] [13]. Open source or drain faults can cause sequential behavior and thus require a certain sequence of patterns in order to be detected. Generally, a sequence of two patterns needs to be applied. The first pattern excites the fault and the second detects it. For example, figure 8 shows a NAND gate with open defect in pMOS transistor source, no current can pass through this transistor. The truth table I shows correct logic results for the first row when the previous value is 0 however the same pattern can not detect the fault when the previous value is 1. The reality is that the  $AB = 01$  vector puts node C in a floating or high-impedance state, and there is no outlet for rapid discharge of its high logic voltage charge from the previous logic state. This one was stored in the load capacitance  $C_L$ . As result, a correct value is read when the previous value is 1 and the fault is detected when previous value is 0.

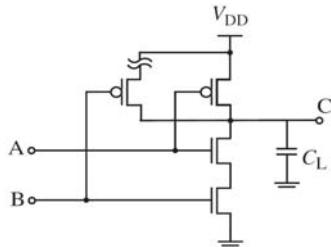


Figure 8. S-D open fault

To simulate this fault all the value of  $R_{OP}$  resistances are replaced by  $1G\Omega$  one at a time and their faulty signatures are then recorded for each location.

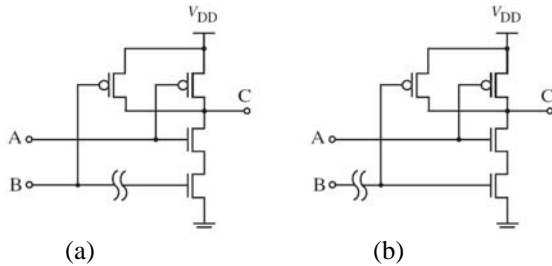


Figure 9. Open gate fault

The second category intra-gate open defects is open gate defect that disconnects one transistor gate (figure 9.a) or more (figure 9.b). The voltage of the floating gate depends on the neighbored lines and parasitic capacitances. In the simulation all the  $R_{OP}$  are deleted one by one and the netlist are simulated with floating lines. The faulty signature is then recorded for each location.

*D. Simulation of resistive open defect*

A resistive-open defect is defined as an imperfect circuit connection that can be modeled as a defective resistor between the circuit nodes that should be connected. In the simulation we replace the value of the resistance  $R_{OP}$  by a resistance of 0.5, 1, 5  $M\Omega$  one at a time and we record the faulty signature. Simulation results show that intra-gate resistive-open faults will cause both slow-to-rise and slow-to-fall faults on the affected node. During stuck-at

fault test, if these defects will be detected they will be detected as stuck-at-0 for the slow-to-rise fault, and will be detected as a stuck-at-1 for the slow-to-fall fault.

V. INTRAGATE FAULT DIAGNOSIS

Fault diagnosis is the process of isolating the source of failure in a defective circuit, so that a physical failure analysis can be performed to physically examine the root cause of failure. Precise diagnosis of different defects affecting chips helps the IC manufacturers to fix the process problems and improve the yield leading to a low cost and shorter time-to-market. The existing logic diagnosis tools [14][15][16][17] can determine, by analyzing the failure's responses, the most likely locations inside a failing die from which the failures originate. These tools allow also the diagnosis of some inter-gate defects such bridging fault and interconnect open defects. However, these tools have limitation to diagnose defects affecting the transistor level.

In the following, we explain our method to diagnose intra-gate defects using the fault dictionary that we have already constructed in the previous section. The method uses the stuck-at fault diagnosis results to determine intra-gate suspect cells then an intra-gate diagnosis algorithm is performed to verify if the real defect is on the interconnecting wire or inside the library cell associated with the identified location.

*A. Localizing potential intra-gate defect from inter-gate diagnosis results*

The stuck-at fault model is the most used fault model in diagnosis. Generally, it is followed by a ranking mechanism to see how close it is to the real defect behavior [16]. The use of these counts can be extended to locate suspect cells with intra-gate defects [20].

Consider the example in figure 10, where two faults were injected. The first one on the interconnect wire between gates  $C2$  and  $C1$ , the second at transistor level inside gate  $C3$ . Table II represents the response of this circuit in presence of these two faults.

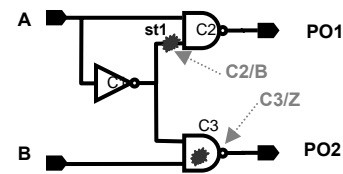


Figure 10. An intra-gate defect in presence of st fault

The inter-gate diagnosis procedure can determine two disjoint defective locations that are not interacting on any primary outputs [25]. The first defect can be modeled by a stuck-at 1 fault. However, the second one cannot be modeled by any inter-gate fault model. The simulation of stuck-at faults (st-1 and st-0), on the output of the faulty location  $C3$ , shows that the combination of these two fault models can explain all the failures caused by this defect. However, several simulation results don't predict the observed responses. For example, the simulation of a st-0 on the output of  $C3$  drives  $PO2$  to 0 for the input value  $(AB=10)$ . However, the test's output  $PO2$  is equal

to 1. Here, we observe the miss-prediction between the simulation results and the observed test responses.

TABLE II. TRUTH TABLE OF THE DEFECTIVE CIRCUIT

	A	B	Tester outputs		Sim (C3/Z st-1)		Sim (C3/Z st-0)	
			PO1	PO2	PO1	PO2	PO1	PO2
0	0	0	1	1/0	1	1	1	1/0
1	0	1	1/0	0/1	1	0/1	1	0
2	1	0	1/0	1	1	1	1	1/0
3	1	1	1	1/0	1	1	1	1/0

Generally, when an intra-gate defect affects a circuit, the simulation of stuck-at fault or combination of stuck-at fault, will explain all its faulty responses, but some simulation results will not match the tester fails.

Figure 11 shows the relation between the Simulation-Fails (SF) obtained while simulating the circuit with an injected fault and the Tester-Fails (TF) from the tester. The relationship between the two sets is captured as diagnostic counts. The failing observe points which are common between TFs and are called Tester Fails-Simulation Fails (TFSF). The observe points, which only fail during simulation are called Tester Pass-Simulation Fails (TPSF). On the contrary, the observe points, which only fail on the tester, are called Tester Fails-Simulation Pass (TFSP).

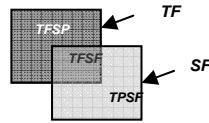


Figure 11. Relation between TF and SF

$$\begin{aligned}
 TF: \{0/PO2, 1/PO1, 1/PO2, 2/PO1, 3/PO2\} & \quad (1) \\
 SF_{st1} (C3/Z): \{1/PO2\} & \quad (2) \\
 SF_{st0} (C3/Z): \{0/PO2, 2/PO2, 3/PO2\} & \quad (3)
 \end{aligned}$$

Consider the same sample in figure 10. The tester fails (1) contains four failing patterns and five failing elements. A failing pattern is defined as a pattern that detects the failures associated with all the primary outputs where the failures were observed. However, a failing element is defined as a failing pattern associated with only one primary output where the failure is observed. The per turn diagnosis applied on this tester fails (1) shows that three of the four failing patterns which constitute this TF are SLAT patterns [26]. Patterns 0 and 3 are explained by the faulty candidate C3/Z, pattern 2 is explained by the faulty candidate C2/B. However, pattern 1 is a Non SLAT failing patterns that can be explained only by the combination of the two faults C3/Z and C2/B. The simulation of a st-1 (2) and st-0 (3) on the output of the failing gate C3 shows that the three fails caused by this defect on the primary output PO2 are explained. However, the simulation of st-0 on the output of C3 shows that {2/PO2} is a passing element belonging to TPSF category. Table III shows the different diagnostic counts for the considered example. As we can observe there are two disjoint cones. Consequently, candidates belonging to each one are not interacting for failing and

passing patterns. So, each candidate in each cone can have its own diagnostic counts.

TABLE III. DIAGNOSTIC COUNTS

Pin name	model	#TFSF	#TFSP	#TPSF
C3/Z	St0	2	1	1
C3/Z	St1	1	2	0
C2/B	St1	2	0	0

An intra-gate defect is diagnosed if all the extracted excitation values on the inputs of the defective cell for its failing and passing patterns are explained by a candidate belonging to the fault dictionary.

To minimize the work space and save computing time, it is important to select the minimum number of cell candidates to be considered in the intra-gate diagnosis algorithm. From the stuck-at diagnosis results, we assign a new TFSF<sub>st01</sub> counts for each failing primary output. This count is the result of adding TFSF<sub>st1</sub> and TFSF<sub>st0</sub> counts. Once this step is performed, we select from each defective cone all the candidates having the biggest TFSF<sub>st01</sub> counts. If more than one candidate exists, we select those having the two lesser TPSF counts as shown in figure 12. For example, experiments on different cells show that:

- When a pattern-dependant defect exists the TPSF<sub>st01</sub> counts will be minimum on the gate's input. Since, the defect can be modeled by a stuck-at fault when the previous pattern excites the defect.
- When an intra-gate bridging fault exists and no stuck at fault on the inputs of the defective cell explains the failures, we found that the TPSF<sub>st01</sub> counts will be lesser on the gate's output.

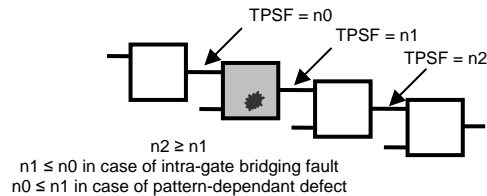


Figure 12. The TPSF counts

B. Determining excitation conditions from patterns with multiple exercising conditions

The exercising conditions are defined as binary logic value combinations that are applied on the input pins of a library cell in the design during the capture phase of a test pattern. To diagnose intra-gate defects these exercising conditions on the input of each candidate cell are determined for both failing and observable passing patterns. However, determining the active excitation conditions values from an industrial design is not a trivial task. Indeed, it may occur that the intra-gate defect is being exercised multiple times in different ways during the capture phase of a test pattern causing multiple exercising conditions [24]. This is due to various reasons like multiple capture cycles, the presence of both leading and trailing edge flops in the design etc.

The following algorithm presents our method to determine active excitation conditions from patterns with multiple exercising conditions.

**Step1:** Collect the exercising conditions on the inputs and outputs of each intra-gate candidate cell.

**Step2:** Divide the exercising conditions values belonging to *failing patterns* into two sub-categories:

- The first one  $SEC_F$  (Single Exercising Conditions) containing only excitation conditions for the failing patterns with single exercising conditions.
- The second one  $MEC_F$  (Multiple Exercising Conditions) containing excitation conditions for the failing patterns with multiple exercising conditions.

**Step3:** Divide the exercising conditions values belonging to *passing patterns* into two sub-categories:

- The first one  $SEC_P$  (Single Exercising Conditions) containing only excitation conditions for the passing patterns with single exercising conditions.
- The second one  $MEC_P$  (Multiple Exercising Conditions) containing excitation conditions for the passing patterns with multiple exercising conditions.

**Step 4:** Remove  $SEC_F$  from  $MEC_P$  and remove  $SEC_P$  from  $MEC_F$ , then repeat step 2 and 3 until no  $SEC_F$  and no  $SEC_P$  exist respectively in  $MEC_P$  and  $MEC_F$ .

**Step 5:** From the fault dictionary find the fault locations matching all the  $SEC_F$  and all the  $SEC_P$

**Step 6:** From the list obtained in step 5 find the candidates that explain one of each  $MEC_P$  and one of each  $MEC_F$ , then rank the candidates according the number of excitation pattern used. The candidate that explains these criteria with minimum input excitation values is more likely to be the good candidate.

For sequence dependant defect, it is mandatory to introduce the previous values in the multiple exercising conditions algorithm.

Consider an example where a NAND gate has been identified as a potential intra-gate defect. The stuck-at fault simulation on the output of this gate shows that patterns P1, P2 and P3 belong to category of failing patterns, and patterns P4 and P5 are passing patterns.

- Input excitation values for P1: {00} → failing pattern
- Input excitation values for P2: {10, 11} → failing pattern
- Input excitation values for P3: {10, 00} → failing pattern
- Input excitation values for P4: {10, 00} → passing pattern
- Input excitation values for P5: {10, 11} → passing pattern

So, for our example, the algorithm will produce the following results: After step 2 and 3, the algorithm will consider pattern P1 as  $SEC_F$ , so {00} is a failing excitation condition. Pattern P2, P3 are considered as  $MEC_F$ , P4 and P5 as  $MEC_P$ . In step 4 {10} is considered as a passing excitation condition and {11} as a failing excitation condition. In Step 5 and 6 we use the fault dictionary to find the fault location that explains this failure.

C. Diagnosis flow

Figure 13 shows the proposed flow of the proposed intra-gate diagnosis algorithm for a failing die.

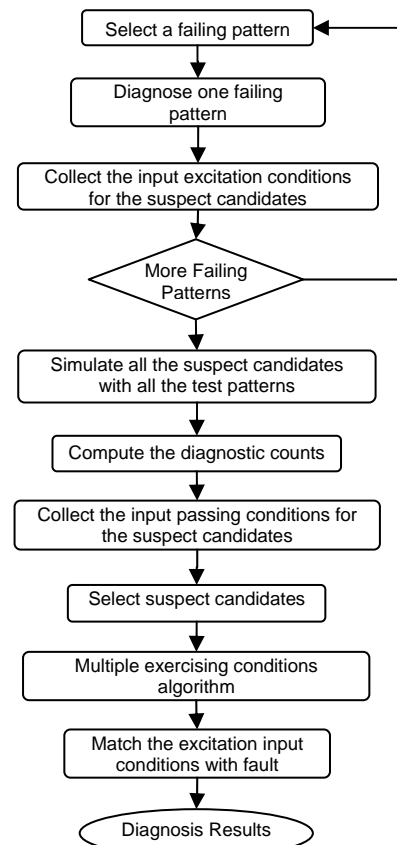


Figure 13. Complete diagnosis flow

Figure 13 shows the proposed flow of the proposed intra-gate diagnosis algorithm for a failing die.

The proposed method begins by selecting one failing pattern from the tester data-log to diagnose it. The input excitation conditions are then collected for each suspect cell. Once all the failing patterns are diagnosed, the suspect cells are simulated with all test patterns. After this step, the diagnostic counts are computed. The input exercising conditions for observable passing patterns are determined. The multiple exercising conditions algorithm is applied to find out the active excitation input values. Finally, the fault dictionary is used to find out the intra-gate defect that matches the failures

VI. EXPERIMENTAL RESULTS

The above methodology was implemented and run on two different libraries to create two different fault dictionaries. Then, we used these data to the intra-gate diagnosis procedure already presented in this paper.

A. Extraction results

TABLE IV. CHARACTERISTICS OF SOME STUDIED GATES

Gate name	Transistor counts	Neighbored shapes counts	Contact counts
HS65_LHS_XNOR2X3	10	19-21	14
HS658_LH_SDFPSQX18	42	112-120	46
HS65_LH_AO222X9	14	29-33	21
HS65_LH_MUX21X4	12	52-23	22
HS65_LH_2X2	4	9-6	9
HS65_LH_AOI222X18	48	23-50	60
HS65_LH_CB4IIX4	10	32-16	16
HS65_LH_NOR4ABX4	10	23-40	15

Table IV shows some characteristics of some gates from ST 65nm library. The second column represents the number of transistors for each of these gates. Column 3 shows respectively the number of neighbored metal shapes and poly-silicon shapes. Column 4 represents the contact counts for each gate.

In the following, we present the detailed results for HS65\_LHS\_XNOR2X3 gate. Figure 14 and 15 represent respectively its layout and its transistor netlist.

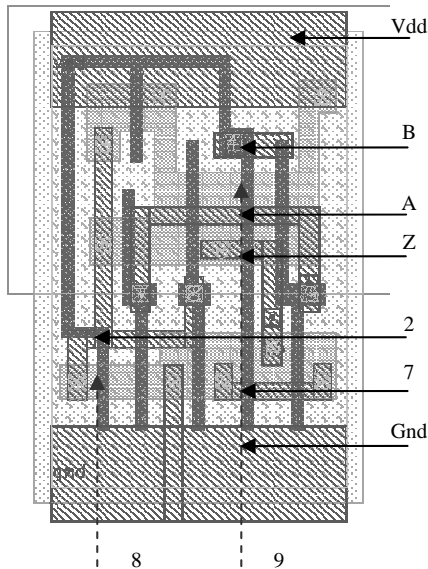


Figure 14. HS65\_LHS\_XNOR2X3 layout

M0 vdd A 2 17 PHVTLP L=0.06 W=0.28 \$X=390 \$Y=1310 \$D=56  
 M1 vdd B 2 17 PHVTLP L=0.06 W=0.28 \$X=430 \$Y=2100 \$D=56  
 M2 Z 2 vdd 17 PHVTLP L=0.06 W=0.55 \$X=735 \$Y=1310 \$D=56  
 M3 9 B Z 17 PHVTLP L=0.06 W=0.55 \$X=1035 \$Y=1310 \$D=56  
 M4 vdd A 9 17 PHVTLP L=0.06 W=0.55 \$X=1225 \$Y=1310 \$D=56  
 M5 8 B 2 18 NHVTLP L=0.06 W=0.2 \$X=250 \$Y=525 \$D=39  
 M6 gnd A 8 18 NHVTLP L=0.06 W=0.2 \$X=460 \$Y=525 \$D=39  
 M7 7 2 gnd 18 NHVTLP L=0.06 W=0.39 \$X=770 \$Y=525 \$D=39  
 M8 Z B 7 18 NHVTLP L=0.06 W=0.39 \$X=1035 \$Y=525 \$D=39  
 M9 7 A Z 18 NHVTLP L=0.06 W=0.39 \$X=1305 \$Y=525 \$D=39

Figure 15. transistor netlist

The extraction of neighbored lines shows that lines 2-Gnd, 2-A, 2-Vdd, Gnd-7, 2-7, 2-Z, 7-Z, A-Z, B-A, B-Vdd, and B-2 are neighbored lines. The extraction of contact locations shows that there are 14 potential open defects.

TABLE V. CONTACT LOCATIONS

Contact name	Net name	transistors
CO1	V <sub>dd</sub>	M4
CO2	V <sub>dd</sub>	M0 M1 M2
CO3	2	M1
CO4	B	M M3 M5 M8
CO5	2	M0
CO6	Z	M2 M3
CO7	A	M0 M6
CO8	2	M2 M7
CO9	A	M4 M9
CO10	Z	M8 M9
CO11	7	M9
CO12	7	M7 M8
CO13	G <sub>nd</sub>	M6 M7
CO14	2	M5

Table V gives the location of the potential open defect for each contact. For example, an open defect on contact CO2 will disconnect V<sub>dd</sub> from M0, M1 and M2 transistors in the same time.

B. Simulation results

Table VI presents the simulation results for intra-gate bridging fault between lines 2 and 7. The simulation results show that the defect drives the gate's output to opposite value for two patterns.

TABLE VI. FAULTY HS65\_LHS\_XNOR2X3 (CASE OF BRIDGE)

A	B	Z <sub>Good</sub>	Z <sub>Faulty</sub>
0	0	1	1
0	1	0	1
1	0	0	1
1	1	1	0

Table VII presents the simulation results for open defect affecting contact CO1 and CO13. The simulation results show that this defect has a different output results according to the output's previous value. The stuck-open fault model is not adequate for the defect affecting CO13 since it disconnects more than one transistor.

TABLE VII. FAULTY HS65\_LHS\_XNOR2X3 (CASE OF OPEN DEFECT)

Z <sub>Previous</sub>	A	B	Z <sub>Good</sub>	Z <sub>CO13</sub>	Z <sub>CO1</sub>
1	0	0	1	1	1
1	0	1	0	1	0
1	1	0	0	1	0
1	1	1	1	1	1
0	0	0	1	1	0
0	0	1	0	1	0
0	1	0	0	1	0
0	1	1	1	1	1

Table VIII presents the simulation results for resistive open defect affecting contact CO13. The simulation results show that the defect can only be observed for the sequences (01) and (10) when the previous value of Z is equal to 1.

TABLE VIII. FAULTY HS65\_LHS\_XNOR2X3 (CASE OF RESISTIVE-OPEN DEFECT)

Z <sub>Previous</sub>	A	B	Z <sub>Good</sub>	Z <sub>CO13</sub>
1	0	0	1	1
1	0	1	0	1
1	1	0	0	1
1	1	1	1	1
0	0	0	1	1
0	0	1	0	0
0	1	0	0	0
0	1	1	1	1

C. Diagnosis results

To verify the effectiveness of the proposed intra-gate fault dictionary developed in this paper, we elaborated controlled experiments in which the behavior of failing chip with an intra-gate fault was simulated. This was performed by injecting intra-gate defects in a list of library cell instances then their fault signature for the whole circuit is recorded.. The method used to simulate intra-gate defects, without a transistor level simulator, consists of replacing the target cells by modified ones in the library netlist. This modified cell represented a defective version of the original cell, by having changed its truth table or behavior. The modified netlist was then simulated against stuck-at test patterns, and the failures

were recorded in data-log. These data-logs are then used in the diagnosis step.

TABLE IX. CIRCUITS STATISTICS

Circuit	Gate count	Gate type count	Pattern #	Scan chains #
A	40	15	14	1
B	382224	777	3131	8

Table IX shows some characteristics of the two circuits used to verify our intra-gate diagnosis approach. The circuit A is a sample circuit with only 40 gates. The circuit B is in production at STMicroelectronics. The second column presents the number of gates in each circuit. The third column shows the number of gate type counts in each circuit. This number is very small comparing to the gate counts which means that the use of fault dictionary is practical since each gate in the circuit is used many times.

### 1) Experiment results for intra-gate bridging faults diagnosis

Table X shows the results for conventional stuck-at diagnosis for 6 intra-gate bridging faults injected in different sample of circuit B. Column 1 shows the suspect intra-gate cells, column 2 represents the number of failing elements on each data-log. Column 3 to 6 indicate the stuck at diagnostic counts on each candidate cell's output.

TABLE X. STUCK-AT FAULTS DIAGNOSIS

Gate name	Stuck-at fault diagnosis				
	TF	TFSF <sub>st0</sub>	TFSF <sub>st1</sub>	TPSF <sub>st0</sub>	TPSF <sub>st1</sub>
F_AN2LLP	2267	1948	319	0	713
AO4ALL	854	125	729	500	0
F_MUX21NLL	1265	0	1265	0	68
F_ND4LL	237	205	32	56	159
OR5HS	331	268	63	524	649
AO7LL	524	295	229	1176	367

Table XI shows the intra-gate diagnosis results obtained by our diagnosis flow on each suspect cell in table X. Column 2 presents the number of suspect transistors on each candidate cell. Columns 3 to 6 show respectively the SEC<sub>F</sub>, MEC<sub>F</sub>, SEC<sub>P</sub> and MEC<sub>P</sub> counts that are used in the multiple exercising conditions algorithm. Column 7 shows the intra-gate bridging fault candidate matching the defect behavior. For example, the cell candidate F\_AN2LLP has 6 transistors. A stuck-at fault on its output explains 86 failing patterns and cause 36 passing patterns. The extraction of exercising conditions on the inputs of this cell shows that 16 of the failing patterns are SEC<sub>F</sub>, however 70 are MEC<sub>F</sub>. In the same way, 24 of the passing pattern cause SEC<sub>P</sub>, however 12 are MEC<sub>P</sub>. Using the fault dictionary, we found a bridging fault between the gate and drain of transistor M<sub>0</sub> explaining this failure.

TABLE XI. INTRA-GATE BRIDGING FAULT DIAGNOSIS

Gate name	Trans	SEC <sub>F</sub>	MEC <sub>F</sub>	SEC <sub>P</sub>	MEC <sub>P</sub>	Defect
F_AN2LLP	6	16	70	24	12	Br G-D M0
AO4ALL	10	29	7	3	2	Br 2-7
F_MUX21NLL	12	23	52	6	23	Br 5-2
F_ND4LL	8	12	4	25	9	Br G-D M5
OR5HS	14	22	105	12	23	Br 9-12
AO7LL	6	36	85	29	8	Br G-D M5

### 2) Experiment results for intra-gate Open defect diagnosis

Table XII shows the corresponding diagnosis results for transistor stuck-open faults. For circuit A, three stuck-open defects were injected on contacts linking a net to many transistors. Unlike bridging fault, excitation of transistor stuck-open fault depends on previous values. Therefore, exercising conditions were collected for previous and current vectors. In all cases, we obtained the good intra-gate candidate that explains the failures. For example, the AO22X4 cell has been identified as suspected cell for intra-gate defect. In fact, all the TF are explained and some TPSF counts exist. This cell contains 10 transistors and 17 contacts. We were able to identify the defective contact using our diagnosis approach.

TABLE XII. INTRA-GATE DIAGNOSIS RESULTS FOR OPEN DEFECT

Gate name	Trans.	Stuck-at diagnosis results			Defect
		TFSF	TFSP	TPSF	
XOR2X4	10	4	0	1	CO2
AO1FX2	8	5	0	3	CO5
AO22X4	10	9	0	2	CO4

Figure 16 represents the layout of the gate AO22X4 that has been diagnosed as defective previously. This gate is from the STMicroelectronics 65nm library. The defective contact CO4 disconnects M1, M3 transistors from M2 and M4 transistors, causing multiple stuck-open defects. Our method was able to diagnose this defect since it is based on the use of physical information whereas other published works fails to identify the correct faulty location.

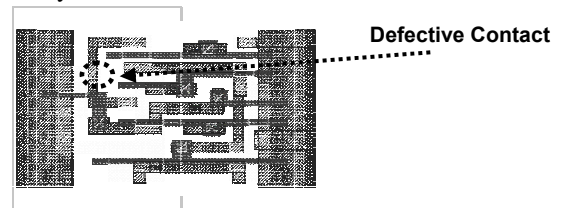


Figure 16. AO22X4's layout

### 3) Experiment results for intra-gate resistive open defect diagnosis

Table XIII shows the corresponding diagnosis results for a NAND2X4 gate with a resistive open defect. The value of the injected resistive open defect is 5 MΩ. Columns 3 to 5 show the stuck-at diagnosis counts, and column 6 shows the defective contact explaining the failures.

TABLE XIII. INTRA-GATE DIAGNOSIS RESULTS FOR RESISTIVE OPEN

Gate name	Trans.	Stuck-at diagnosis results			Defect
		TFSF <sub>st01</sub>	TFSP <sub>st01</sub>	TPSF <sub>st01</sub>	
NAND2X4	4	4	0	3	CO1

## VII. CONCLUSION

In this paper, we have presented a method to automate the extraction and the simulation of intra-gate defects affecting standard cell library. The proposed method uses the verification CAD tools calibre and SVRF rule file to extract potential intra-gate defect. All the extracted

defects are then simulated one at a time using Eldo simulator then recorded in an intra-gate fault dictionary. These data are used to diagnose intra-gate defects affecting standard cell libraries. Experimental results in controlled simulated environment prove the effectiveness and accuracy of our method in isolating the injected defect using fault dictionary.

## REFERENCES

- [1] J. Li, C.W. Tsang E.J. McCluskey "Testing for Resistive Opens and Stuck Opens" Proc, Int Test Conf 2001 pp 1049-1058.
- [2] S. T. Zachariah and S Chakravarty "Extraction of Two-Node Bridges From Large Industrial Circuits" IEEE Trans CAD 2004 pp 433- 439.
- [3] D. Walker and Z. Stanojevic "FedEx: Fast-bridging fault extractor," in Proc. IEEE Test Conf., 2001 pp. 696-703.
- [4] C. Di and J. Jess, "On accurate modeling and efficient simulation of CMOS opens," in Proc. Int. Test Conf., Baltimore, MD, 1993 pp. 857-882.
- [5] J. Li et al, "Diagnosis for Sequence Dependent Chips", VLSI Test Symposium, 2002, pp.187-192.
- [6] V. Champac, A. Rubio, and J. Figueras, "Electrical Model of the floating gate defect in CMOS IC's: Implications on IDDQ Testing" IEEE Trans on CAD 94 pp 359-356.
- [7] A. Ladhar, L. Bouzaida, and M. Masmoudi "Layout Based Method to Diagnose Intra-gate Defects in Presence of Multiple-Fault" in Proc of IEEE SCS conference, 2008
- [8] A. Ladhar, L. Bouzaida, and M. Masmoudi "Efficient and Accurate Method to Diagnose Intra-gate Defects in Nanometer Technology and Volume Data" in Proc of DATE conference, 2009
- [9] Mentor graphics documentation, "Standard Verification Rule Format (SVRF) Manual", Calibre v2007.4
- [10] Mentor graphics documentation "Calibre Query Server Manual", Calibre v2007.4
- [11] Mentor graphics documentation "Eldo's user Manual" Eldo v2007.2
- [12] HP. Kuan X.M. Zhang "Physical analysis of TiSi2 bridging (gate-to-S/D) failure in IC" Proc IPFA Singapore, IEEE 2005.
- [13] S.M. Menon, et al "Testable Design of BiCMOS Circuits for Stuck-Open Fault Detection using Single Patterns" VLSI Test Symposium, April 1993. pp. 296-302.
- [14] J. A. Waicukauski and E. Lindbloom, "Failure Diagnosis of Structured VLSI", in IEEE Design and Test of Computers, Aug. 1989, pp 49-60.
- [15] S. Venkataraman and S. B. Drummonds, "POIROT: A Logic Fault Diagnosis Tool and Its Applications", in Proc. of Inter. Test conf. 2000, pp 253-262.
- [16] C. Hora et al, "On Electrical Fault Diagnosis tool in full-scan circuits", in Workshop on Defect Based Testing, 2001, pp 17-22.
- [17] W. Zou et al, "On Methods to Improve Location Based Logic Diagnosis ", in Proc. VLSI Design, 2006, pp 181-187.
- [18] X. Fan et al, "A Novel Stuck-at Based Method for Transistor Stuck-Open Fault Diagnosis", in Proc. of International Test Conference 2005, paper 16.1
- [19] X. Fan et al, "A gate Level Method for Transistor-Level Bridging Fault Diagnosis" in Proc. Of VLSI Test Symp. 2006, pp 266-271.
- [20] X. Fan et al, "Extending Gate-Level Diagnosis Tools to CMOS Intra-Gate Faults", in Trans. In Silicon Debug and Diagnosis 2007 pp 685-693
- [21] E. Amyeen and al "Improving Precision Using Mixed Level Fault Diagnosis" in Proc. of Inter. Test conf. 2006 paper 22.3
- [22] J. Li and E. J. McCluskey "Diagnosis of Resistive-Open and Stuck-Open Defects in Digital CMOS ICs" in Trans. On Computer aided Design, 2005 pp 1748-1759.
- [23] R. Desineni et al "A Logic Diagnosis Methodology for Improved localization and Extraction of Accurate defect Behavior" in Proc. of Inter. Test conf. 2006.
- [24] M. Sharma et al, "Faster Defect localization in Nanometer Technology based on Defective Cell Diagnosis" in Proc. of Inter. Test conf. 2007 paper 15.3
- [25] [12] Z. Wang et al "An Efficient and Effective Methodology on the Multiple Fault Diagnosis" in Proc. of Inter. Test conf. 2003 pp. 329-338
- [26] T. Bartenstein, D. Heaberlin, L. Huisman, and D. Sliwinski, "Diagnosing combinational logic design using the single location at-a-time (slat) paradigm," in Proc. of Inter. Test conf. 2001, pp. 287-296.
- [27] A. Ladhar, M. Masmoudi, and L. Bouzaida "Extraction and Simulation of Potential Bridging Faults and Open Defects Affecting Standard Cell Libraries" in Proc of IEEE SCS conference, 2008



**Aymen Ladhar** was born in Sfax, Tunisia. He received the diploma in Electrical engineering and M.Sc. degrees in Electronics from the University of Sfax, in 2006 and 2007, respectively. He is currently working toward the Ph. D. degree at the University of Sfax, Tunisia.

His research works during B.Sc. M.Sc. and Ph. D degrees are done in STMicroelectronics. They include fault diagnosis, logic debugging, and layout analysis.



**Mohamed Masmoudi** was born in Sfax, Tunisia, in 1961. He received the Electrical engineering degree from National Engineering School of Sfax in 1985 and the Ph. D degree in microelectronics from the Laboratory of Computer Sciences, Robotics and Microelectronics of Montpellier, Montpellier, France in 1989.

From 1989 to 1994, he was an Associate professor with the National Engineers School of Monastir, Tunisia. Since 1995, he has been with the National Engineering School of Sfax, where, since 1999, he has been a Professor engaged in developing microelectronics in the engineering program of the university, and where is also the head of the Laboratory Electronics, Micro-technology and Communication. He is the author and coauthor of several papers in the microelectronics field. He has been a reviewer for several journals.

Prof. Masmoudi organized several international conferences, and has served on several technical program committees.